24th Mediterranean Conference on Control and Automation (MED)
June 21-24, 2016, Athens, Greece

On Robotic Impact Docking for On Orbit Servicing*

Zisos Mitros, *Student Member, IEEE,* Iosif S. Paraskevas, *Member, IEEE* and Evangelos G. Papadopoulos, *Senior Member, IEEE*

Abstract— **On-orbit servicing missions will rely on space robots; however their complexity requires prior careful studies. Among these, robotic docking is especially challenging. In this work, the robotic impact docking between two space systems is considered. The impedance properties required to design an impedance controller are studied. These properties include the ratio of the masses between the systems under impact, the relative stiffness between the bodies of each space system and the associated damping factor. The velocity of the probe tip to be commanded is calculated aiming at successful latch at first impact. Simulation results validate the proposed approach.**

I. Introduction

On-Orbit Servicing (OOS) missions such as satellite servicing and refueling, construction of large assemblies, and space debris removal and mitigation will be of critical importance in the near future. The use of space robotic systems in such missions is a viable approach and attracts increased interest; however, their complexity requires prior careful studies. Space agencies worldwide dedicate a significant amount of their budget to OOS and run missions such as the ETS-VII, the Robotic Refueling Mission (RRM), and the Clean Space. A critical aspect of these is reaching and capturing a target, i.e. another satellite or debris. This task includes the phases of far and close rendezvous, and mating i.e. docking or berthing.

Mating to a target, see Figure 1, is a demanding task due to impacts and dynamic coupling [1]. Docking and capturing procedures are associated with impact forces applied when two space systems come into contact. The difficulty of this task increases when the systems have comparable masses. Recent works study the problem taking into account the system dynamics, either post impact, [2], or prior to impact, [3]. The concept of virtual mass and impedance control were proposed and studied in order to tackle the problem [4].

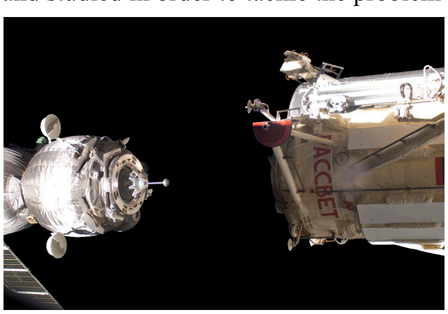

Figure 1. Probe - Drogue Docking System.

More specifically in the case of passive docking (*impact docking*), to accomplish the task the two systems, called *Chaser* and *Target*, have to come into contact, so that impact forces develop. These forces can lead to system separation or damage of critical subsystems. Hence it is necessary to model the impact adequately and study the effects of mass and compliance parameters during latching, so that a controller for successful docking can be developed [5].

To study these impacts, many modeling approaches have been proposed [6]. As the computational power in space is limited, while the impact is a fast process, simplified but relatively accurate models are necessary. Furthermore, a method that could predict the performance prior to impact could produce useful results for tuning the gains of a selected controller. In the literature one can find approaches that can lead to chaotic responses, not to mention the ambiguous problem of multiple impacts, [7], [8]. Considering the above issues, lumped parameter models constitute a useful approach, applied mainly to cases of rigid impacting bodies, [9], [10]. However, the use of lumped parameters is useful also in designing impedance filters and controllers.

A docking procedure was proposed in [11]; however, the importance of having all systems floating and not rigidly fixed was neglected; hence the obtained simulation results involve inaccuracies compared to a realistic scenario. Using a Hardware-In-the-Loop (HIL) simulator, a method to set the compliance during an impact equal to that in an experiment, was proposed, [12]. However, the time delay introduced set limits to system parameters and the associated system stability, leading to a small range of values suitable for experiments. The high robot stiffness causes a contact duration shorter than the time to compute the robot dynamics. This time delay adds energy to the system, which may lead to inconsistencies in the simulation results, instability of the closed-loop system, or damages in the HIL system. The authors tried to minimize but did not eliminate the time delay, and proposed a stability analysis for a range of stiffness and damping properties, [13].

In this paper our previous work on multibody impact docking is extended [14]. The impedance properties required to design an impedance controller are studied. These include the mass ratio of the systems under impact, the relative stiffness between the bodies of each space system and the associated damping factor. The velocity of the probe is calculated aiming at a successful latching during the first impact. Simulation results validate the proposed approach.

II. Scenario and System Modeling

To prevent a faulty satellite from becoming space debris, a robotic system (Chaser) will have to dock on it (Target) using a dedicated latching system and then perform an OOS task. The type of latching docking system of interest here is similar to the Russian Probe-Drogue Docking System, employed at the International Space Station (ISS), see Figure 1. In more

* The authors are with the School of Mechanical Engineering, National Technical University of Athens, 9 Heroon Polytechneiou Str., 15780 Athens, Greece. (e-mail: mitroszisis@gmail.com; isparas@mail.ntua.gr; egpapado@central.ntua.gr; ph.: +30-210-772-1440).

978-1-4673-8345-5/16/$31.00 ©2016 IEEE

detail, the Chaser is composed of a free-floating spacecraft base, a manipulator and a probe, see Figure 2a. The probe mechanism is connected to the manipulator, which is mounted to the base. The Target includes a drogue with a latching mechanism, connected flexibly to its satellite base. The parameters of the Target are known, but those of the Chaser can be modified for optimum response. This can be simplified and studied in 2D, see Figure 2b, where the Chaser and the Target are moving along the same (x-) axis. The aim here is to study the behavior of the interaction and then control it; therefore, a single-axis analysis is undertaken (central impact), as is common in the literature [1].

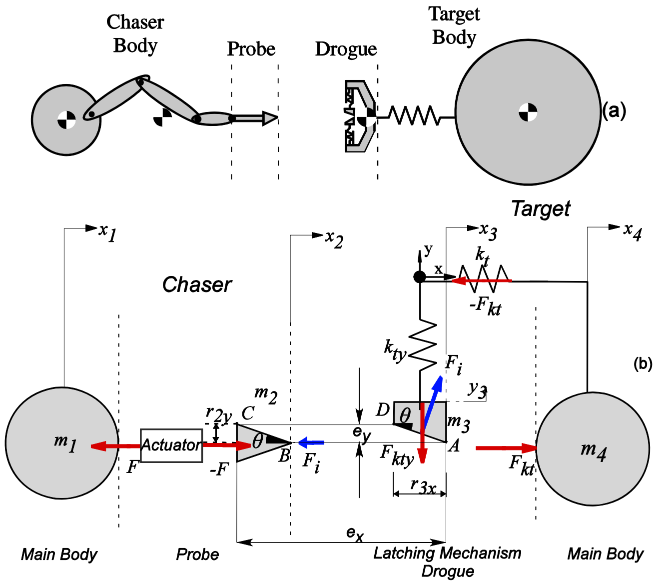

Figure 2. Model of impact docking: (a) Two floating spacecrafts, one equipped with a manipulator, and (b) A simplified system model.

Multibody systems under impact can be modeled as two-body systems; this approach is known as an equivalent two-body system model, i.e. an "n" multibody system under impact, can be modeled as a two-body system with one body being equivalent to the first k masses, and the second body equivalent to the rest $n - k$ masses, connected by equivalent spring/damper elements [15]. A Chaser space robot (parent) comprises a main body, flexible appendages (e.g. antennas, solar panels), and an articulated robotic manipulator. Without introducing significant errors, the base and the small masses located away from the impact point are lumped to a larger mass m_1 in one end (main body in Figure 2b), with a probe of mass m_2 in the other. They are connected through an actuator acting as a spring-damper system, whose compliance characteristics can be set by control. The Chaser main body center of mass (CoM) position is denoted by x_1 and the position of the probe tip by x_2, see Figure 2b. The position of the CoM of the Chaser parent system, $x_{c,cm}$ is given by

$$x_{c,cm} = (m_1 x_1 + m_2 x_2)(m_1 + m_2)^{-1} \tag{1}$$

The Target parent consists of a base of mass m_4, whose CoM position is described by x_4, and is connected to the drogue of mass m_3 whose point A position is described by x_3, see Figure 2b. The position of CoM of the Target parent system, $x_{T,cm}$ is given by an equation similar to (1). The spring k_t models the flexibility of the drogue-base connection. The drogue latch includes a compliant element with spring constant k_{ty}, which is compressed during an impact, see Figure 2b. If the probe tip (point C) can fully overshoot the latching mechanism (point A), the later returns to its initial position, securing the probe. Whenever $x_2 < x_3$, no impact occurs. The drogue is assumed to be symmetrical, therefore a single y-axis spring is used, with its spring constant corresponding to the equivalent stiffness of all latching mechanism springs.

Without loss of generality, the Target has zero velocity and the Chaser has an initial constant velocity $\dot{x}_{1,0} = \dot{x}_{2,0}$. At the moment t_i at which the impact occurs, the masses m_2 and m_3 have the same position, i.e. $x_2 = x_3$. Then, the probe starts pushing the latching mechanism, and for the duration of the contact, the latch spring k_{ty} is being compressed. The system equations of motion, obtained after the contact between m_2 and m_3, are given by:

$$\begin{aligned}
&m_1\ddot{x}_1 = -F_c \\
&m_2\ddot{x}_2 = -F_{i,x} + F_c \\
&m_3\ddot{x}_3 = F_{i,x} - k_t[l_0^{'} - (x_4 - x_3)], \quad t_i \le t \le t_i + t_{imp} \\
&m_3\ddot{y}_3 = F_{i,y} - k_{ty}[l_0^{"} + y_3] \\
&m_4\ddot{x}_4 = k_t[l_0^{'} - (x_4 - x_3)]
\end{aligned} \tag{2}$$

where F_c is the controlled force applied on the probe, $l_0^{'}$, $l_0^{"}$ are the free lengths of springs k_t and k_{ty} respectively, and $F_{i,x}$, $F_{i,y}$ are the impact forces between the probe and drogue. All forces are shown in Figure 2b.

For successful latching, the interaction force can be controlled by an impedance controller with appropriate parameters. To design such a controller, an impedance filter describing the desired impact behavior is selected first as:

$$F_{i,x} = m_f(\ddot{x}_2 - \ddot{x}_1) + b_f(\dot{x}_2 - \dot{x}_1) + k_f(x_2 - x_1) \tag{3}$$

where m_f, k_f, b_f are mass, spring and damper design parameters to be determined. Using (2) and (3) to achieve this impedance behavior, the applied actuator force F_c must be,

$$\begin{aligned}
F_c = F_{i,x}\Big(((m_f/m_2 - 1)\mu_{c,ef})/m_f\Big) + \\
+\mu_{c,ef} b_f(\dot{x}_2 - \dot{x}_1)/m_f + \mu_{c,ef} k_f(x_2 - x_1)/m_f
\end{aligned} \tag{4}$$

where $\mu_{c,ef}$ is the effective mass of the Chaser,

$$\mu_{c,ef} = m_1 m_2 / (m_1 + m_2) \tag{5}$$

The m_f is selected equal to m_2 so that F_c does not depend on $F_{i,x}$. Then, the applied actuator force F_c becomes,

$$F_c = k_d(\dot{x}_2 - \dot{x}_1) + k_p(x_2 - x_1) \tag{6}$$

where k_d, k_p are controller gains given by,

$$k_d = b_f \mu_{c,ef}/m_2, \; k_p = k_f \mu_{c,ef}/m_2 \tag{7}$$

Impact Modeling. The description of the impact forces is developed using viscoelastic theory. According to this theory, a compliant surface under impact can be modeled by a combination of lumped parameter elements, i.e. by springs and dampers. Common impact models include the Kelvin-Voigt (KV) and the Hunt-Crossley (HC) model, [6]. For example, the interaction force F_g using the KV model is

$$F_g(y_g, \dot{y}_g) = k_g y_g + b_g \dot{y}_g \tag{8}$$

where k_g and b_g are the stiffness and damping coefficients of the impact respectively and y_g the penetration of one body in the other. Using (8) in (2) and assuming that the impact is elastic (no damping), the impact force, see Figure 3, becomes,

$$\begin{aligned} F_{i,x} &= K_i(x_2 - x_3) \\ F_{i,y} &= F_{i,x} / \tan(\theta) \end{aligned} \quad , \quad \theta > 0 \tag{9}$$

where K_i is the fictious impact spring.

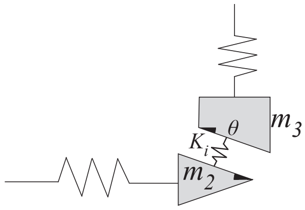

Figure 3 Impact model for impact docking model.

In many cases, it is useful to model the impact as part of a harmonic motion. More specifically, an impact has two phases, compression and restitution. These can be modeled as the half-period of a sinusoidal motion with period T_{imp}; the smaller the duration of impact, the better the approximation. In fact, for impact durations of less than 1 s, this approach yields very good results, as it also incorporates the effects of energy losses; however for very small durations, these effects are generally negligible. Thus, the duration of this high frequency oscillatory motion is

$$t_{imp} = T_{imp}/2 = \pi\sqrt{\mu_{i,ef}/K_i} \tag{10}$$

where $\mu_{i,ef}$ is the effective mass of the bodies under impact,

$$\mu_{i,ef} = m_2 m_3/(m_2 + m_3) \tag{11}$$

Using (10), one can estimate for how much time (2) is valid. When m_2 and m_3 are not in contact, (2) applies with zero impact force.

Description of Impact during Simulations. According to the previous analysis, the impact docking model described in this work depends on the relative position of the systems. Although, the time that the bodies are in contact is given by (10), the use of (2) for more than a single impact is not considered. For (2) to be valid again, and taking into account Figure 2, two requirements must be met:

- The lines that pass from points A, D and B, C respectively must coincide.
- Point A must belong to the line segment BC.

Equivalently, the following inequalities must be fulfilled simultaneously:

$$0 < x_2 - x_3 < r_{3x} \tag{12}$$

$$0 < y_3 - y_2 < r_{2y} \tag{13}$$

$$y_2 + \tan(\theta)x_2 = y_3 + \tan(\theta)x_3 \tag{14}$$

where r_{2y} and r_{3x} are geometric features, see Figure 2.

III. Estimation of Impedance Parameters

To achieve latching during impact docking, the impedance parameters m_f, k_f, b_f for the implementation of the impedance filter must be selected. One can identify three requirements necessary to have a successful latch, which in turn will allow the estimation of these parameters.

1st Requirement: Impedance mass, $m_f = m_2$.

As mentioned above, we choose $m_f = m_2$ so that a force sensor will not be necessary for the computation of the actuator force. Because of that, selecting the appropriate m_2 is important for implementing the impedance filter. An analytical method for setting m_2 is developed here.

The displacement during an impact can be approximated by a partial harmonic motion. The impulse developed along the x-axis $P_{imp,x}$ during impact is given by,

$$P_{imp,x} = \left(1 + e^*\right) U^-_{relx,i} \mu_{i,ef} \tag{15}$$

where $U^{i-}_{relx,i}$ is the relative velocity of the bodies under impact on the x-axis, hence the subscript (i). The superscript (-) stands for the velocity prior to an impact, while e^* is the *Coefficient of Restitution* (CoR), see also [7]. The relative velocity between the systems $U^{i\pm}_{relx,s}$ where the subscript (s) stands for both masses m_c and m_t, before (-) or after impact (+) occurred at moment t_i can be defined as

$$U^{i\pm}_{relx,s} = \dot{x}^{i\pm}_{c,cm} - \dot{x}^{i\pm}_{t,cm} \tag{16}$$

where $\dot{x}^{i\pm}_{j,cm}$, $j = c,t$ is the absolute velocity of the Chaser (c) or the Target (t) parents CoM before or after the impact with respect to the inertial frame as given by, (1). Since the same impulse $P_{imp,x}$ is developed between the Chaser and Target, and between the two masses under impact (m_2 and m_3), as parts of their parent systems (Chaser or Target), and since this impulse represents a momentum exchange,

$$P_{imp,x} = m_c\left(\dot{x}^{i-}_{c,cm,x} - \dot{x}^{i+}_{c,cm,x}\right) \tag{17}$$

$$P_{imp,x} = m_t\left(\dot{x}^{i-}_{t,cm,x} - \dot{x}^{i+}_{t,cm,x}\right) \tag{18}$$

where m_c, m_t are the total masses for the Chaser and Target parent systems respectively. Therefore, the post-impact Chaser and Target CoM relative velocities are

$$\begin{aligned} U^{i+}_{relx,s} &= \dot{x}^{i+}_{c,cm,x} - \dot{x}^{i+}_{t,cm,x} = \\ &= \left(\dot{x}^{i-}_{c,cm,x} - P_{imp,x}/m_c\right) - \left(\dot{x}^{i-}_{t,cm,x} + P_{imp,x}/m_t\right) = \\ &= \left(\dot{x}^{i-}_{c,cm,x} - \dot{x}^{i-}_{t,cm,x}\right) - P_{imp,x}\left(1/m_c + 1/m_t\right) \\ &\Rightarrow U^{i+}_{relx,s} = U^{i-}_{relx,s} - P_{imp,x}/m_{i,ef} \end{aligned} \tag{19}$$

where the total system effective mass, $m_{i,ef}$ is given by

$$m_{i,ef} = m_c m_t/(m_c + m_t) \tag{20}$$

After some manipulation and using (15), it can be found that

$$U^+_{relx,s} = \left(1 - e^*_I\right) U^-_{relx,s} \tag{21}$$

where

$$e^*_I = \left(1 + e^*\right) e_I \tag{22}$$

and where e_I is defined by

$$e_I = \mu_{i,ef}/m_{i,ef} \tag{23}$$

and called the *Coefficient of the Effective Masses*. Based on the value of the coefficient e_I, one can determine whether the Chaser will continue, stop or change its direction of motion, after the impact as it sets the sign of $U^+_{relx,s}$. The following cases can be clearly identified, when $e^* = 1$ (elastic impact):

(i) $e_I = 0 \Rightarrow U^+_{relx,s} = U^-_{relx,s}$: No impact occurs.

(ii) $e_I = 1 \Rightarrow \mu_{i,ef} = m_{i,ef} \Rightarrow U^+_{relx,s} = -U^-_{relx,s}$: Resembles an elastic impact between two rigid bodies. The relative velocity between the two systems is equal to the relative velocity of two rigid bodies as $m_2 \gg m_1$ and $m_3 \gg m_4$.

(iii) $e_I = 1/2 \Rightarrow U^+_{relx,s} = 0$: The two parent systems move with the same velocity.

(iv) $0 < e_I < 1/2 \Rightarrow U^{+}_{relx,s} U^{-}_{relx,s} > 0$: The two parent systems move in the same direction after impact. The Chaser continues its motion, while the Target moves in the Chaser's direction, at lower speed. This is the *favorable case* for latch.

(v) $1/2 < e_I < 1 \Rightarrow U^{+}_{relx,s} U^{-}_{relx,s} < 0$: The two systems move in different directions. The Chaser reverses its direction of motion, and the Target moves towards the initial direction of the Chaser. *This prevents latching.*

The previous results show that the behavior during impact depends on the *mass ratios*, and not on the mass values. In the case that the Target's masses and mass m_1 are known, one can find the mass of the Chaser's probe m_2 that enables latch, i.e. one that ensures $0 < e_I < 1/2$. Many interesting cases corresponding to different ratios of masses are presented in [14]. This value can be used for example to select which joints to lock and which joint to operate during docking, at a manipulator with many degrees of freedom so as to achieve the desired m_2 and hence the impedance parameter m_f.

2[nd] Requirement: Minimum Impact Velocity for Latching.
The second requirement is related to the minimum impact velocity of the probe for successful penetration. To achieve latching, the force due to the impact must be such that the latching part of the Target's drogue is compressed to the height of the probe tip, denoted by r_{2y} in Figure 2b. The motion of m_3 also depends on the spring k_{ty} force (and its damping if it is considered).

More specifically, the maximum elongation $u_{\max}$ of the y-axis spring attached to m_3, must be larger than the height of the probe tip. This requirement can be described by

$$u_{\max} \geq r_{2y} \tag{24}$$

The compression of m_3 is maximum when its velocity is zero. Then the kinetic energy transforms into potential energy and

$$k_{ty} u_{\max}^2 \big/ 2 = P_{imp,y} \mu_{t,ef} \big/ 2 m_3^2 \Rightarrow u_{\max} = P_{imp,y} \Big/ \left(m_3 \sqrt{k_{ty} / \mu_{t,ef}} \right) \tag{25}$$

where $P_{imp,y}$ is the impulse along the y-axis, given by,

$$P_{imp,y} = (1 + e^{*}) U^{i-}_{relx,s} \mu_{i,ef} \tan(\theta) \tag{26}$$

and $\mu_{t,ef}$ is the Target effective mass, defined by,

$$\mu_{t,ef} = m_3 m_4 / (m_3 + m_4) \tag{27}$$

Using (24)-(26), the relative velocity $U^{i-}_{relx,s}$ for successful latching is found to be:

$$U^{i-}_{relx,s} \geq \frac{m_3 r_{2y} \tan\theta}{(1 + e^{*}) \mu_{i,ef}} \sqrt{\frac{k_{ty}}{\mu_{t,ef}}} \tag{28}$$

As can be seen using (28), for larger Target drogue mass m_3, or for higher stiffness k_{ty}, higher impact velocity is necessary to compress the latching mechanism by the latching distance r_{2y}. As e^{*}, the impact velocity must be increased further. This is in accordance to experience.

3[rd] Requirement: Impedance Parameters k_f, b_f.
As the Target stiffnesses are assumed known, the impedance filter stiffness k_f and damping b_f must be selected. An analytical solution for the selection of these coefficients is difficult to be obtained because of the large number of parameters involved. To investigate possible solutions with the minimum impact velocity for latching, the analytical model of a Chaser and a Target was developed, where various parameters (masses, stiffnesses, velocities, etc.) can be varied.

The two systems were simulated when coming into contact and the success or failure of latching was noted. An algorithm was developed to search the range of Chaser gains for Target stiffnesses k_t between $300 - 700\,N/m$. The remaining parameters were $m_1 = 1500\,kg$, $m_4 = 2000\,kg$, $k_{ty} = 100\,N/m$, while the masses under impact, m_2, m_3, varied between $20 - 40\,kg$.

Figure 4 displays the ratio k_f / k_t as a function of the known Target stiffness k_t and allows selecting the appropriate impedance parameter k_f. The larger the Target stiffness is, the smaller the k_f must be, so that the force acting on mass m_1 is small. Due to the small force and the fact that m_1 ? m_2, the probe will continue its motion into the drogue despite the impact force.

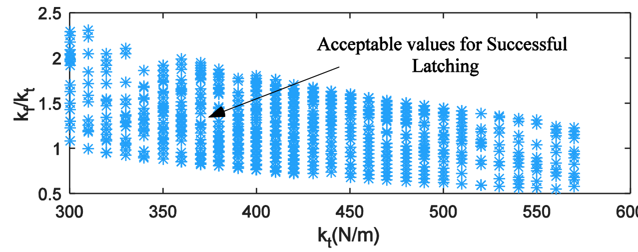

Figure 4. Impedance parameter k_f vs. k_t for successful latching.

Having selected the impedance filter mass and stiffness parameters of the Chaser, one can calculate the impedance damping too. Choosing critical damping results in,

$$b_f = 2\sqrt{m_f k_f} \tag{29}$$

Having selected $m_f = m_2$, k_f and b_f, the controller gains given by (7) can be calculated.

IV. Simulation Results

To examine the validity of the analysis, a series of simulations using MATLAB/Simulink were run. The Target has been modeled as a two mass and spring system, while the Chaser as an impedance-controlled two-mass system. The contact forces between the bodies under impact were calculated using the KV model; the impact was modeled by a spring, which can only be compressed. As the simulation advances, the velocities of the masses under impact are calculated, as well as their interpenetration. This is fed back to the contact model and a force is developed which pushes away the masses under impact. Therefore, prior to and after the impact, the simulation presents two moving two-body systems, and during impact a four-body system.

To avoid bias of the results, no equation stemming from the theoretical analysis in this work was used in the simulation. The user can also change the initial parameters of the bodies. The initial velocity of the Chaser masses m_1 and m_2 before impact are nonzero and equal. All other initial conditions have been set to zero without loss of generality.

Validation of the effect of the coefficient e_I. To examine the effect of e_I on the post-impact behavior, a simulation was run in which the m_f is chosen such that $1/2 < e_I < 1$. For this choice, it is expected that no latching will occur.

The parameters used are those of case A in Table 1. According to (23) the coefficient of the effective masses is $e_I = 0.9809$. The initial position of m_2 is $x_{2,0} = -0.3m$ and for m_3 is $x_{3,0} = 0.3m$. As Figure 5b shows, the Target-Chaser relative position e_x decreases until the moment in which the impact occurs. However, due to the poor choice of the mass ratio, the systems after the impact move in different directions and docking fails; Figure 5a validates this fact.

Table 1. Data for simulation runs.

Properties	A	B	C	D	E	F
m_1 (kg)	40	17	10	5	100	1500
m_2 (kg)	1500	2	10	50	20	40
m_3 (kg)	2000	1.5	10	10	10	20
m_4 (kg)	20	15	10	100	200	2000
k_i (N/m)	10^5	15000	15000	15000	15000	10^5
k_f (N/m)	513	100	1000	1000	1000	513
k_t (N/m)	370	200	200	200	200	370

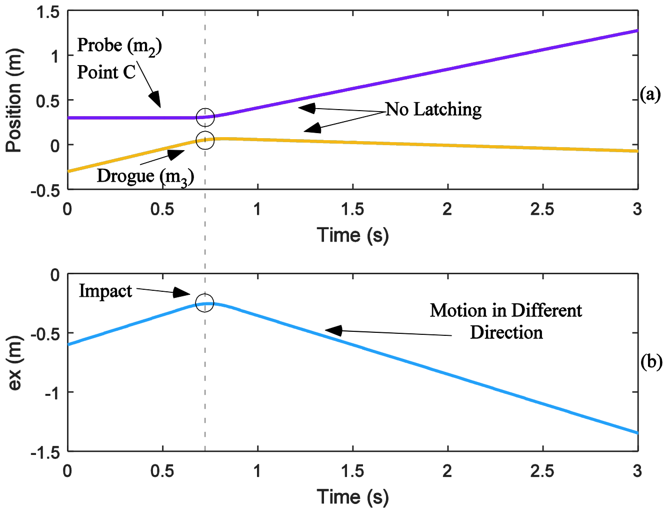

Figure 5 (a) Positions of probe-drogue – (b) Relative positions in the case that e_I is not appropriate for successful docking.

For successful docking, the impedance mass $m_f = m_2$ is chosen as a function of the known Target masses and the main mass of the Chaser robot. To do this, (23) is employed to plot e_I against the Target mass ratio for a constant Chaser mass ratio, see Figure 6. For a given Target mass ratio and a desired coefficient e_I, one can find the Chaser mass ratio, and since m_1 is known, m_2 and $m_f = m_2$ are selected. For example, using case F in Table 1 and considering all the parameters as inputs expect of the mass m_2 i.e. $m_4 / m_3 = 100$ and for $e_I < 0.02$, Figure 6 yields $m_1 / m_2 = 1500/40$. Since $m_1 = 1500 kg$, then it follows that $m_f = m_2 = 40 kg$.

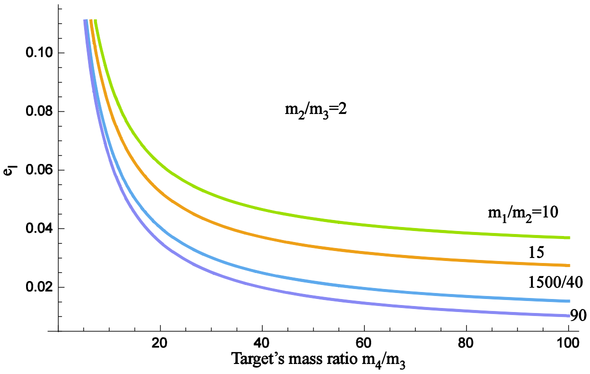

Figure 6. The e_I vs the Target mass ratio, for Chaser mass ratios.

To verify the analysis for the post-impact relative velocity between the Chaser and the Target as a function of the pre-impact relative velocity, and thus the validity of (21), various configurations (B, C, D, and E) were examined, see Table 1. In all cases, the theoretical model calculates the post-impact relative velocity with high accuracy as compared to simulation results, as shown in Table 2.

Table 2. Simulation results for validation of e_I using (21).

	B	C	D	E
Initial Rel. Velocity	0.05	0.05	0.05	0.05
Final Rel. Velocity using Eq. (21) (m/s)	0.0403	0	0.02728	0.0413
Final Rel. Velocity (by simulation) (m/s)	0.0402	-0.000476	0.02715	0.0412
Absolute Error (m/s)	0.0001	0.000476	0.00013	0.0001

Minimum velocity for impact docking. Using as an example case F in Table 1 and (28), the minimum velocity is calculated to be $U^{i-}_{relx,s} = 0.5031\, m/s$. If the Chaser relative velocity is lower than this value, then, the developed impulse during the first impact is not enough for complete latching with one impact between the probe and the latch mechanism. For example, if we choose $U^{i-}_{relx,s} = 0.303 m/s < 0.5031 m/s$ and apply the first impact impulse to m_3, this is displaced without exceeding the mechanism threshold, see Figure 7a; therefore no latching will occur.

On the other hand, if multiple impacts are allowed, then the latching mechanism may be compressed fully thanks to additional impacts; however this is an undesirable design due to the uncertainty involved. Figure 7b displays the case with $U^{i-}_{relx,s} = 0.303 m/s < 0.5031 m/s$. Two impacts occur and latching is successful. However, this case is not desirable as mentioned above.

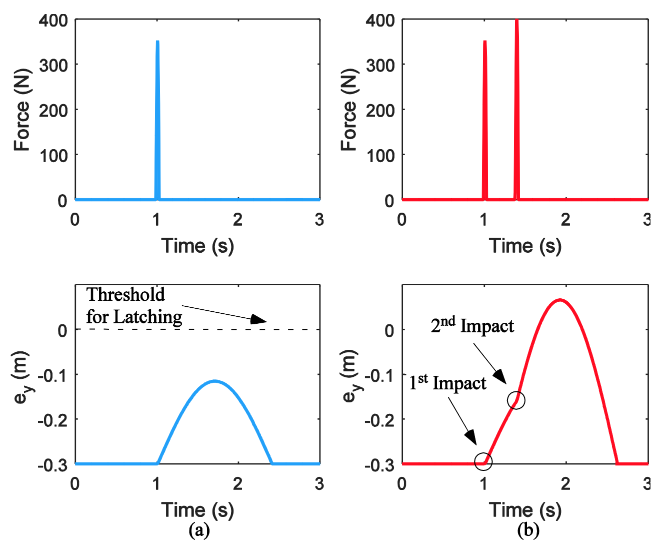

Figure 7. Impact for $U^{i-}_{relx,s} = 0.303\ m/s < 0.5031\ m/s$. (a) Taking into account the first impact only, (b) multiple impacts.

Fulfillment of all Conditions. As an example, we use case F in Table 1, and select $m_f = 40kg$, as explained earlier. The stiffness of the impedance filter is chosen from Figure 4 for a specific value of Target stiffness. Assuming this stiffness to be $k_t = 360 N/m$, i.e. a common value for the flexibility between the drogue and the Target main body, the impedance parameters should be $k_f = 513.3 N/m$ (computed and given in Table 1), and $b_f = 282.8 Ns/m$, (computed using (29)). As a result, using (7), the gains of the controller are found to be $k_p = 500\, N/m$ and $k_d = 279\, Ns/m$. It is assumed that the impact is elastic, $e^* = 1$. Before the impact, point A is at $y_3 = -r_{2y}$; to be compressed enough so that the probe tip can be inserted, it must reach $y_3 = 0$. To achieve this, (28) yields the minimum initial relative velocity as $U^-_{relx,s} = 0.503 m/s$. This relatively high velocity indicates the difficulty of performing robotic docking in space. As shown in Figure 8a, a single impact for docking is necessary, during which the probe and latching mechanism are in contact continuously. As shown in Figure 8b, the actuator force and commanded by the controller is smooth, and reasonable in magnitude, while due to the selection of critical damping, the closed-loop cyclical frequency is 3.58 rad/s and the applied actuator force settles in $1.6 s$, as expected.

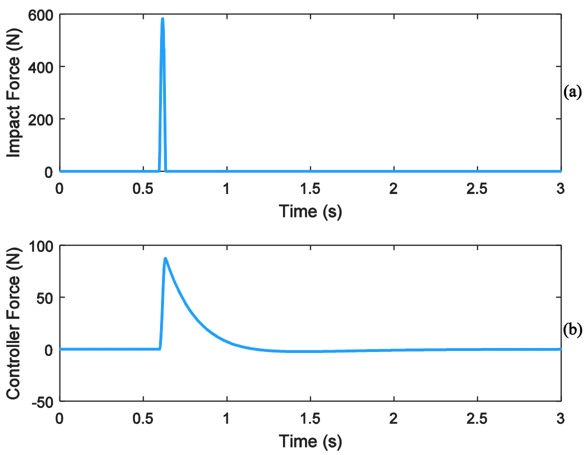

Figure 8. (a) Impact force and (b) actuator force acting on the probe.

Figure 9 shows the positions of the Chaser and the Target, their relative positions, and the y-axis position of m_3. When $x_2 = x_3$, an impact occurs. The spring k_{ty} starts being compressed while the Target starts moving in the x-axis as a system. Bodies m_2, m_3 oscillate because of the impact force and also move in the x-axis as they are connected with the larger masses m_1, m_4 whose oscillations are negligible.

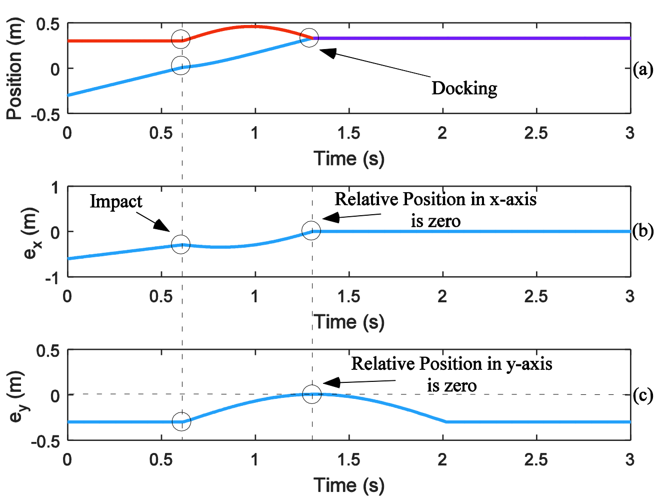

Figure 9. (a) Position of probe (Chaser) and drogue (Target). - Relative Position of Chaser- Target (b) in the x-axis and (c) in the y-axis.

Latching is considered to be successful when points A and C (see Figure 2) acquire the same position in both axes. It can be seen from Figure 9 that when the Chaser has the minimum velocity as given by (28), m_3 is compressed so as to reach the position of point C (relative position along y-axis is zeroed). At the same time, the x-axis relative position of m_2 and m_3 is also zeroed and latching is successful. Mass m_3 returns to its original position following a successful latch, see Figure 9c.

V. Conclusion

The robotic impact docking between two space systems was considered. The conditions for successful docking were studied analytically. The effect of the ratio of masses between multibody systems during impact was developed and the effect of the stiffness ratio between them was analyzed. The minimum impact velocity for successful latch between a Chaser robotics system and a Target satellite has been calculated. An impedance controller was used to control the chaser manipulator and a methodology for choosing its parameters for successful docking was developed. Simulations validated the developed analysis.

References

[1] Fehse, W. (2003). *Automated Rendezvous and Docking of Spacecraft*, Cambridge University Press, ISBN 9780521089869.

[2] Dimitrov, D. N., and Yoshida, K. (2004). "Momentum distribution in a space manipulator for facilitating the post-impact control," *Int. Conf. on Intelligent Robots and Systems*, Sendai, Japan, pp. 3345-3350.

[3] Ma, O, Flores-Abad, A., and Pham, K. (2012). "Control of a Space Robot for Capturing a Tumbling Object," *Int. Symp. on Artificial Intelligence, Robotics & Automation in Space*, i-SAIRAS. Turin, Italy.

[4] Yoshida, K., and Nakanishi, H. (2003) "Impedance Matching in Capturing a Satellite by a Space Robot," *Int. Conf. on Intelligent Robots and Systems*, Las Vegas, Nevada, pp. 3059-3064.

[5] Yoshida, K., et al (2004) "Dynamics, control and impedance matching for robotic capture of a non-cooperative satellite" *Advanced Robotics*, 18(2), pp. 175-198.

[6] Gilardi, G. and Sharf, I. (2002). "Literature Survey of Contact Dynamics Modelling," *Mech. & Machine Th.*, 37(10), pp. 1213-1239.

[7] Quinn, D. D., and Bairavarasu, K. (2006). "Near simultaneous impacts," *Int. Journal of Impact Engineering*, 32(6), 889–904.

[8] Jia, Y.-B., Mason, M. T., and Erdmann, M. A. (2012). "Multiple impacts: A state transition diagram approach," *The International Journal of Robotics Research*, 32(1), pp. 84–114.

[9] Stronge, W. J. (2000). *Impact Mechanics*, Cambridge University Press, ISBN 9780521602891.

[10] Brach, R. M. (1991). *Mechanical Impact Dynamics – Rigid Body Collisions*, John Wiley & Sons.

[11] Uyama, N., Y. Fujii, K. Nagaoka, and K. Yoshida. (2012). "Experimental Evaluation of Contact/ Impact Dynamics Between Space Robot with a Compliant Wrist and Free-Flying Object," in *Int. Symp. on AI, Robotics and Automation in Space (i-SAIRAS).*

[12] Zebenay, T. Boge, R. Lampariello, D. Choukroun, (2013), "Satellite Docking Simulator based on Hardware-In-the-Loop Hybrid Contact Model" *12th Symposium on Advanced Space Technologies in Robotics and Automation, (ASTRA '13),* ESA, ESTEC, The Netherlands.

[13] Zebenay, M., T. Boge, D. Choukroun., (2014), "Modeling, Stability Analysis, and Testing of a Hybrid Docking Simulator," *Acta Astronautica, 00*, 1-30.

[14] Paraskevas, I., Mitros, Z., and Papadopoulos, E., (2015), "On Inertia and Stiffness Effects During Impact Docking" *13th Symp. on Advanced Space Technology in Robotics and Automation, (ASTRA '15),* ESTEC, The Netherlands.

[15] Xu, W. et al, (2015), "A Practical and Effective Method for Identifying the Complete Inertia Parameters of Space Robots," *IEEE/RSJ Int. Conf. on Intelligent Robots and Systems (IROS 15),* Hamburg, Germany, pp. 5435 – 5440.